COUPLED THM ANALYSIS OF LONG-TERM ANISOTROPIC CONVERGENCE IN THE FULL-SCALE MICRO TUNNEL EXCAVATED IN THE CALLOVO-OXFORDIAN ARGILLITE

TOURCHI, S.*, VAUNAT, J.* GENS, A.*, VU, M.N† , BUMBIELER, F†

*Department of Geotechnical Engineering and Geosciences
Universidad Politècnica de Catalunya (UPC)
Campus Norte UPC, 08034 Barcelona, Spain

e-mail: saeed.tourchi@upc.edu
† National Radioactive Waste Management Agency (Andra),
1 rue Jean Monnet, 92290 Châtenay-Malabry

Key words: in situ testing; numerical modelling; convergence measurements; anisotropy.

Abstract. The main purpose of this paper is to analyse the convergence measurements of the ALC1604 in situ heating test carried out in the Callovo-Oxfordian claystone formation (COx) in the Meuse/Haute-Marne underground research laboratory (MHM URL). The concept of the test consists of horizontal micro-tunnel, equipped with a steel casing. The micro-tunnel is excavated in the direction of the horizontal principal major stress (σ_H). In situ observations showed anisotropic convergence with the maximum and minimum values in the horizontal and vertical directions, respectively. Coupled THM numerical analyses have been carried out to provide a structured framework for interpretation, and to enhance understanding of THM behaviour of Callovo-Oxfordian claystone. However, a special mechanical constitutive law is adopted for the description of the time-dependent anisotropic behaviour of the COx. The simulation of the test using this enhanced model provides a satisfactory reproduction of the THM long-term anisotropic convergence results. It also provides a better understanding of the observed test response.

1 INTRODUCTION

The construction of the M/HM URL was initiated by the French National Radioactive Waste Management Agency (Andra) in 2000 with the main objective of demonstrating the feasibility of geological repository of radioactive waste in the Callovo-Oxfordian claystone formation. It has indeed very favourable characteristics for radioactive waste disposal like low permeability, significant retardation properties for radionuclide migration, no economic value and often exhibits a significant capacity of hydraulic self-sealing of fractures. A network of experimental drifts has been excavated in the directions of the horizontal principal stresses. Micro-tunnels were excavated from these experimental drifts to test the feasibility of disposal cells for packages of high-level radioactive waste and their impact on the surrounding rock.

The HA-ALC1604 is an in situ heating test conducted in the M/HM URL at the main 490 m deep level (Armand et al. 2017). The concept of the test consists of horizontal micro-tunnel approximately 25 m long and 0.7 m in diameter which has been excavated in the direction of the major horizontal stress. The excavation rate of the micro-tunnel was around 0.3-0.5 mh^{-1} and the

excavation was completed in seven days. A non-alloy steel casing was placed in the cell body while the cell head was sustained by a metal sleeve called the Insert. **Figure 1** shows the concept of the experiment, with the 25m long micro-tunnel and surrounding boreholes for THM observations. Five heaters (H1 to H5), each 3 m long and 0.5 m in diameter, have been installed in the body section. The power applied in the deepest 15m was constant and equal to 220 W/m, in order to reach around 85 ºC in two years.

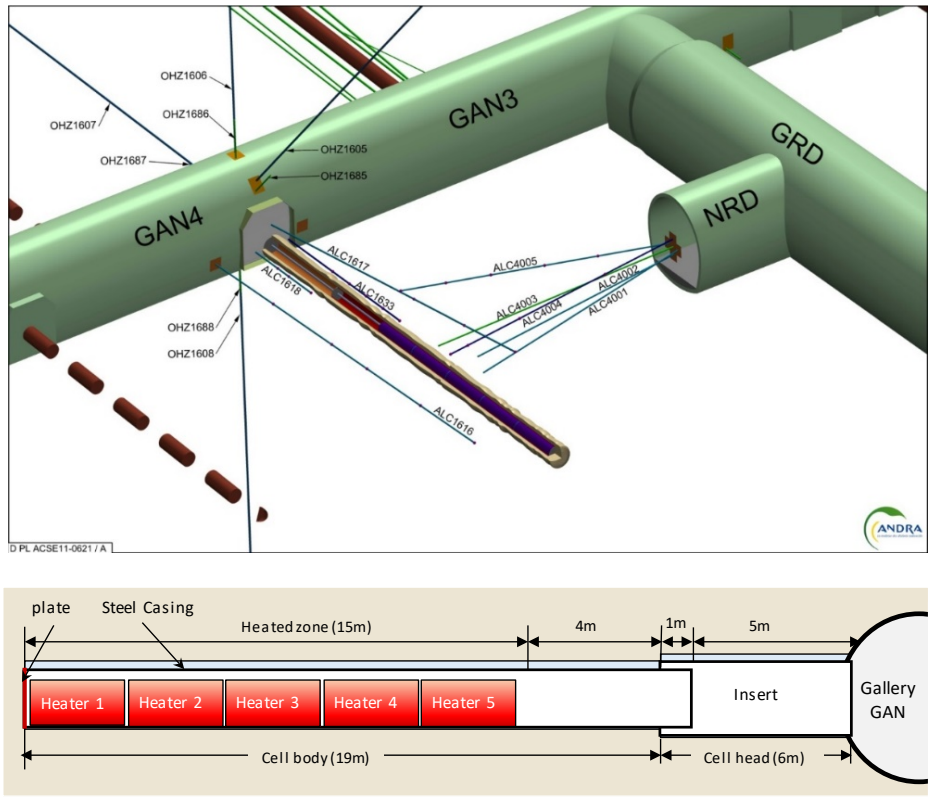

Figure 1 General scheme of the HA-ALC1604 is an in situ heating test.

2 MAIN FEATURES OF THE NUMERICAL MODEL

The coupled THM formulation employed herein to the solution of the analyzed boundary value problem is a particular case of the general formulation presented in Olivella et al. (1994). However, a special mechanical constitutive law is adopted for the description of the stress-strain behaviour of the Callovo-Oxfordian claystone. It has been presented in more detail in (Mánica; et al. (2016a) and Mánica et al. (2016b)). The model was developed within the framework of elastoplasticity and includes a number of features that are relevant for a satisfactory description of COx hydromechanical behaviour: anisotropy of strength and stiffness, behaviour nonlinearity and occurrence of plastic strains prior to peak strength, significant softening after the peak, time-dependent creep deformations and permeability increase due to damage (Gens 2011). Both saturated and unsaturated conditions are considered. The mesh and main boundary conditions (BC) are illustrated in **Figure 2**. The model includes the host rock domain, the steel casings and the gap between the casings, the container and the COx. For computational purposes, the gap will be dealt with as a continuous medium provided with the bi-linear elastic model to represent opening and closing responses. According to the experimental set-up, the casing is supported at the bottom of

the excavation. Thus, container, gaps and casing are eccentric with respect to the centerline of the micro-tunnel. The specific parameters used in the analysis are listed in Table 1-3.

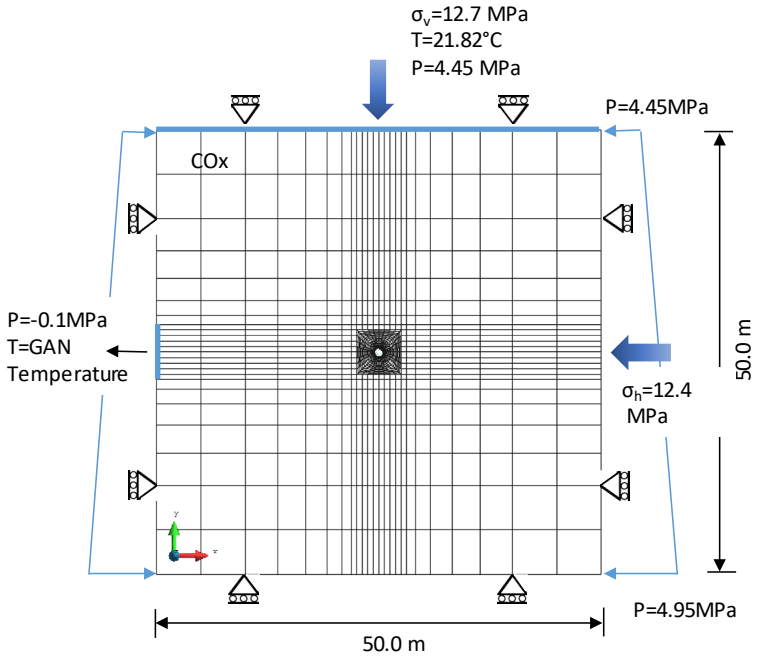

Figure 2 Finite element mesh and boundary conditions.

Table 1 Callovo-Oxfordian claystone parameters used in the 2D THM analysis.

properties	Parameter	Orientation*	Value
Physical	Porosity, ϕ	-	15
Thermal	Thermal Conductivity, λ: W/m/K	Parallel	2.05
		Perpendicular	1.33
	Specific Heat of Solid, cs: J/kg/K	-	800
Hydraulic	Intrinsic Permeability, k	Parallel	6·10-20
		Perpendicular	3·10-20
Mechanical	Young's Modulus, E: MPa	Parallel	5200
		Perpendicular	4000
	Poisson ratio, ν	Parallel	0.25
		Perpendicular	0.35
	Solid compressibility, βs	-	2.5·10-5
HM coupling	Biot Coefficient, b	-	0.6
TM coupling	Linear Thermal expansion coefficient of the rock, αT: K-1	-	1.4·10-5
	Linear Thermal expansion coefficient of the solid grain, bs: K-1	-	1.4·10-5

Table 2 Steel casing properties adopted in the 2D THM analysis.

properties	Parameter	Value
Thermal	Thermal Conductivity, λ : (W/m/K)	80
	Specific heat of solid (J/kg/K)	550
	Linear Thermal expansion coefficient, α_T: K^{-1}	$1.4 \cdot 10^{-5}$
Mechanical	Young's Modulus, *E*: MPa	0.005
	Poisson's ratio, ν (-)	0.3

Table 3 Air-gap element properties adopted in the 2D THM analysis.

properties	Parameter	Value
Thermal	Thermal Conductivity, λ_{dry} : (W/m/K)	0.035
	Thermal Conductivity, λ_{sat} : (W/m/K)	0.6
Hydraulic	Intrinsic permeability, k_0 : (m2)	10^{-16}
	Porosity, ϕ_0 (-)	0.8
	Parameter for van Genuchten model, λ (-)	0.5
	$P_0(\phi) = P_0 \exp\left[\alpha(\phi_0 - \phi)\right]$, $P_0(MPa)$	0.001
	Parameter for van Genuchten model, *a* (-)	10
Mechanical	Young's Modulus, E_c: MPa	1000
	Young's Modulus, E_o: MPa	1.0
	Strain limit, $\varepsilon_{v\,\mathrm{limit}}$ (-)	0.005
	Poisson's ratio, ν (-)	0.3

3 NUMERICAL SIMULATION AND INTERPRETATION

3.1 Excavation damage zone

The experiments have revealed that excavation operations induce damage and fracturing around the galleries (Armand et al. 2014), creating a zone known as the excavation damaged zone (EDZ), where significant changes in flow and transport properties take place (Tsang et al. 2005). The observed configuration of the EDZ depends on the orientation of the excavation with respect to the anisotropic in situ stress state. The EDZ is identified as one of the key issues affecting the long-term behaviour of the tunnel near-field (Blümling et al. 2007). Major efforts have been made to simulate these experimental excavations (Seyedi and Gens 2017) and to gain insights into the design of the actual repository. As stated above, the ALC1604 cell is parallel to the major horizontal stress σ_H has a nearly isotropic stress state in the plane normal to the tunnel axis. However, the EDZ extends further in the horizontal direction (***Figure 3***a), suggesting strong anisotropic characteristics of the rock mass. An estimate of the configuration of the excavation damaged zone can be obtained by plotting contours of the cumulative plastic multiplier as it is directly related to the magnitude of irreversible strains (***Figure 3***b). The lateral extent of the shear fractures zone for smaller opening is almost equal to 1 diameter of the opening (Armand et al. 2014). Model results suggest that a plastic zone of up to 0.7 m away from the micro-tunnel wall is formed. In the zones of the higher plastic multiplier, greater mechanical effects will be noticed on the deformability of rock and hydraulic diffusion. It can be seen that the configuration of the damaged zone is similar to that observed in the previous micro-tunnels with the same orientation, extending more in the horizontal direction (Armand et al. 2014, 2017).

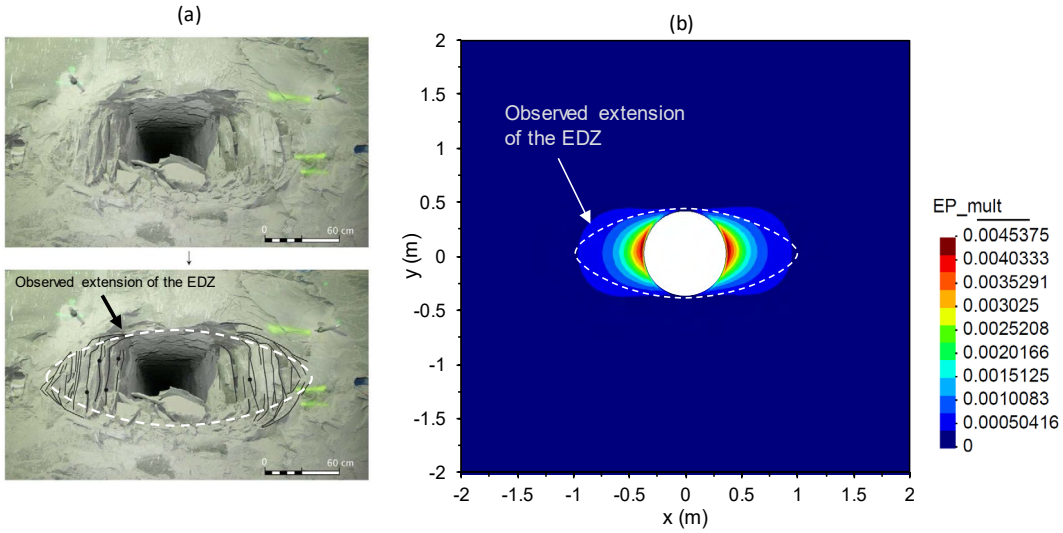

Figure 3 (a) Extension of the damaged zone around a full-scale HLW cell parallel to major horizontal stress (b) Obtained configuration of the EDZ in terms of the plastic multiplier in the cross-section-1 at the end of excavation.

3-1- Convergence Measurements

Figure 5 shows the overall evolution of convergence measurement in steel casing section 9, at a depth of 7 m, and insert sections 11 and 12, at respective depths of 4 and 2m in the cell (note that the sensors were connected 48 days after the excavation of the micro-tunnel). Although the in-situ stress field is isotropic in the section of a micro-tunnel parallel to σ_H, measurements exhibit an anisotropic load. This behaviour is consistent with the convergence anisotropy measurements reported by Morel et al. (2013) and Armand et al. (2013).

With regard to the steel casing, three loading stages can be distinguished in ***Figure 5***a. In the first one, the load is localized in the horizontal direction, corresponding to the maximum extension of the excavation-induced fracture network. It can be observed that immediately after emplacement, the casing starts to converge in the horizontal direction, meaning that the theoretical initial annular space, which is about 3 per cent of the excavation diameter, is totally consumed in this direction in less than 25 days. This loading results in the radial bending of the casing and decrease in diameter. The heating phase strongly increases the casing convergence rate and thus the casing deformation, until contact with the micro-tunnel vault occurs. In this step, the ovalization of the casing continues until it reaches the rock wall in the vertical direction. Once the annular space is closed in the vertical direction, the mechanical load remains anisotropic with no impact on the casing convergence.

The second loading step is followed by a third one, corresponding to a progressive decrease of the load anisotropy, resulting in a decrease of the ovalization. After one year heating, convergence rate is less than 5. 10^{-11} s^{-1}, which is the same order of magnitude as convergence rate of 5 m in diameter, drifts having the same orientation (Armand et al. 2013). ***Figure 5b,5c*** present the horizontal and vertical convergence of Insert sections 11 and 12. A similar short-term mechanical loading of the casing is observed also at the insert. However, after 5 years of measurements, the convergence of the insert is not stabilized, which means that we are still in the first loading step as defined before. The behaviour of the insert sections does not show any significant heating impact (the sections were 8 and 6 meters behind the heated zone). On both sections, the loading schema is the reverse of that seen for the sleeve and consists of vertical convergence and noticeably

equivalent horizontal divergence. Given that, the annular space is much smaller at the insert level (initially 12 mm at the radius, compared with 25 mm around the casing), this behaviour could be caused by the insert being in contact with the rock in the vertical and horizontal planes. As the mechanical strength of the rock was lower horizontally due to the damage generated during excavation, the insert tended to diverge horizontally. For both sections, the loading direction is rotated with respect to the previous one and characterized by a vertical convergence and noticeably equivalent horizontal divergence. A comparison between the results of the analysis and observations, in terms of diameter variations (measured on the casing at the depth of 7 m and on the insert at a depth of 4 and 2m) are presented in ***Figure 5***. It is apparent that the evolution and maximum convergence is reasonably well captured with the formulation and parameters used.

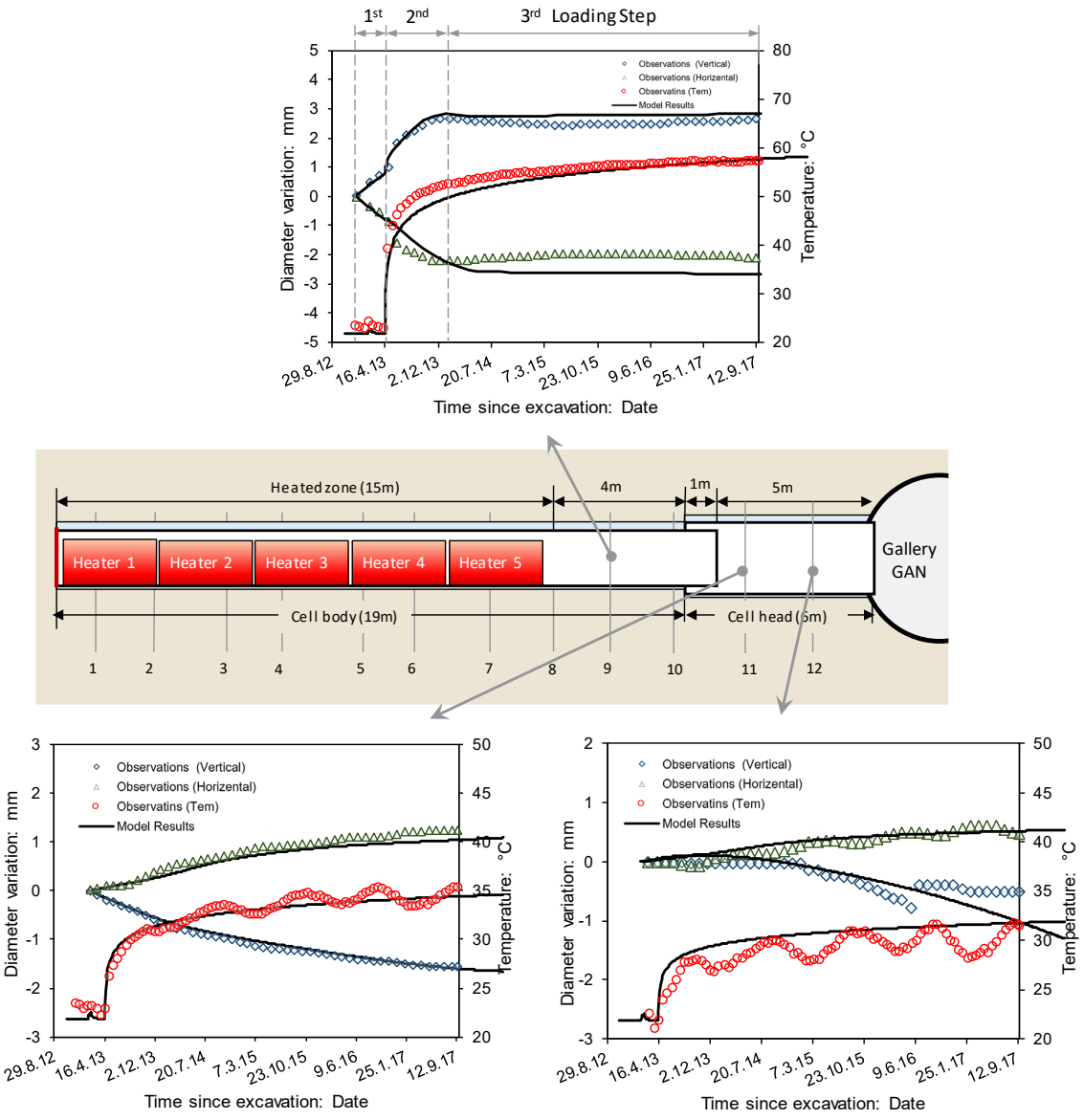

Figure 4 Diameter variations measured on the sleeve at a depth of 7 m and on the insert at a depth of 4 and 2 m (negative values = convergence)

5-2- Mechanical signatures

The strain gauges were glued on the casing previously to its installation and connected 27 days after the cell was excavated. For each section, the gauges are spread out into six sectors, two in the horizontal plane and the other four at 45° angles on either side of it. ***Figure 5*** presents the evolution of the circumferential strain ($\varepsilon_{\theta\theta}$) around the inner face of the casing at different times and at 18 m depth (section 4) with the computed results from the analysis. These evolutions tend towards a stabilized curve, which represents the mechanical signature of the applied load. Indeed casing does not evolve significantly after the second year of heating. By comparison with the numerical results, the maximum load direction corresponds to an inclination of 30° with respect to the horizontal.

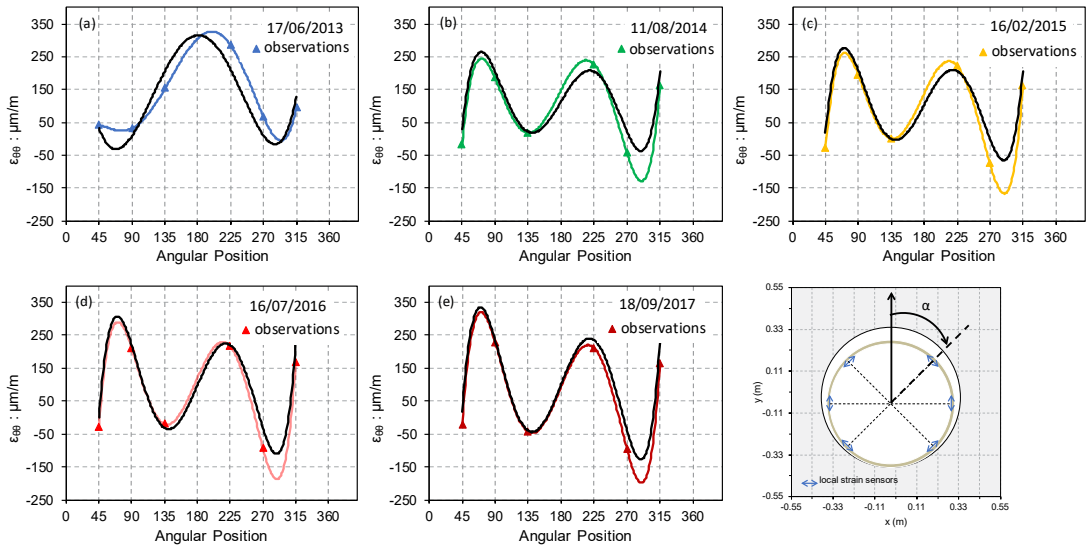

Figure 5 Evolution of circumferential strain at 18m depth for (a) 17/06/2013 (b) 11/08/2014 (c) 16/02/2015 (d) 16/07/2015 (e) 16/07/2016 (f) 18/09/206.

4 CONCLUSIONS

The HA-ALC1604 in situ heating test performed by Andra was modelled using the finite-element code Code_Bright. The mechanical behaviour of the material has been described by a constitutive model that explicitly developed for this type of material. It is of interest to note that the predicted damaged zone appears to be quite consistent with the test observations. Overall, the theoretical formulation adopted and the analysis performed have been able to provide a satisfactory reproduction of in situ test observations, even from a quantitative point of view.

We analysed convergence measurements in HA-ALC1604 test in Callovo-Oxfordian claystone, with the axis following the direction of the major initial principal horizontal stress. The first convergence measurement was made several days after the end of excavation and thus the analysis of the recorded data mainly focused on the time-dependent behaviour of the rock formation. The in situ measurements showed an anisotropic closure of the walls that evolved over time. The analysis of in situ deformation as measured in the full-scale test has led to the definition of the short-term mechanical load applied by the rock. Three loading steps can be distinguished for casing parallel to the major horizontal stress:

1) The localized load applied along the horizontal direction;

2) Significant anisotropic load with no impact on the convergence once the casing reaches the vault of the borehole;

3) Progressive decrease of the load anisotropy.

The applied load remains anisotropic after more than 5 years. This phenomenon is explained by the specific elliptic shape of the excavation-induced fracture network, which governs the convergence of the cell wall. ***Figure 3*** presented qualitatively the extension of this damaged zone around an uncased full-scale cell. The heating effect has been highlighted concerning the duration of the first loading step. Indeed steps 2 and 3 have only been reached on the steel casing (after one year) in the heated zone. At insert sections, the insert remains in the first loading step after 5 years of measurements. The bending stiffness is the same for both, casing and insert this difference is mainly related to heating phase in step 2 as shown in ***Figure 4***. Strain gauges measurements performed on ALC1604 cell have shown anisotropic loading applied by the rock, which is almost horizontal.

REFERENCES

[1] Armand G, Bumbieler F, Conil N, et al (2017) Main outcomes from in situ thermo-hydro-mechanical experiments programme to demonstrate feasibility of radioactive high-level waste disposal in the Callovo-Oxfordian claystone. 1–13. doi: 10.1016/j.jrmge.2017.03.004

[2] Armand G, Leveau F, Nussbaum C, et al (2014) Geometry and properties of the excavation-induced fractures at the meuse/haute-marne URL drifts. Rock Mechanics and Rock Engineering 47:21–41. doi: 10.1007/s00603-012-0339-6

[3] Blümling P, Bernier F, Lebon P, Derek Martin C (2007) The excavation damaged zone in clay formations time-dependent behaviour and influence on performance assessment. Physics and Chemistry of the Earth 32:588–599. doi: 10.1016/j.pce.2006.04.034

[4] Gens A (2011) On the hydromechanical behaviour of argillaceous hard soils-weak rocks (Keynote Lecture). In: Geotechnics of Hard Soils – Weak Rocks, Proceedings of the 15th European Conference on Soil Mechanics and Geotechnical Engineering. Thomas Telford, London, pp 71–118

[5] Mánica M, Gens A, Vaunat J, Ruiz DF (2016) A cross-anisotropic formulation for elasto-plastic models. Geotechnique 1–7

[6] Miguel Mánica;, Gens; A, Vaunat; J, Ruiz DF (2016) A time-dependent anisotropic model for argillaceous rocks . Application to an underground excavation in Callovo-Oxfordian claystone. Computers and Geotechnics. doi: 10.1016/j.compgeo.2016.11.004

[7] Olivella S, Carrera J, Gens; A, Alonso E (1994) Non-isothermal multiphase flow of brine and gas through saline media. Transport in Porous Media 15:271–293

[8] Tsang CF, Bernier F, Davies C (2005) Geohydromechanical processes in the Excavation Damaged Zone in crystalline rock, rock salt, and indurated and plastic clays - In the context of radioactive waste disposal. International Journal of Rock Mechanics and Mining Sciences 42:109–125. doi: 10.1016/j.ijrmms.2004.08.003